九州大学学術情報リポジトリ
Kyushu University Institutional Repository

加算平均OCT Angiographyを用いた網膜毛細血管瘤の描出

海津, 嘉弘

https://hdl.handle.net/2324/4110402

出版情報：九州大学, 2020, 博士（医学）, 課程博士
バージョン：
権利関係：(c) 2019 by the American Academy of Ophthalmology Published by Elsevier Inc.

KYUSHU UNIVERSITY

AMERICAN ACADEMY OF OPHTHALMOLOGY®

Microaneurysm Imaging Using Multiple En Face OCT Angiography Image Averaging

Morphology and Visualization

Yoshihiro Kaizu, MD,[1] Shintaro Nakao, MD, PhD,[1] Iori Wada, MD,[1] Mitsuru Arima, MD, PhD,[1] Muneo Yamaguchi, MD, PhD,[1] Keijiro Ishikawa, MD, PhD,[1] Masato Akiyama, MD, PhD,[1] Junji Kishimoto, PhD,[2] Toshio Hisatomi, MD, PhD,[1] Koh-Hei Sonoda, MD, PhD[1]

Purpose: In diabetic retinopathy (DR), OCT angiography (OCTA) could not image all fluorescein angiography (FA)-detected microaneurysms. We investigated whether multiple image averaging could enhance the microaneurysm detection capability of OCTA in patients with DR.

Design: Prospective and cross-sectional observational study.

Participants: Consecutive 31 patients (n = 62 eyes) with DR.

Methods: All eyes underwent FA and 3 × 3 mm fovea-centered OCTA images were obtained using 2 devices: RTVue XR Avanti (Optovue Inc, Fremont, CA) and OCT HS-100 (Canon Inc, Toyko, Japan). OCTA imaging (HS-100) was performed 10 consecutive times. Microaneurysm detection capability was compared among 5 OCTA images (single image, ×3, ×5, and ×10 averaged images and single scan image with the RTVue XR Avanti device).

Main Outcome Measures: Microaneurysm detection capability and the correlation between microaneurysm clinical characteristics or morphology and the extent of image averaging required for OCTA detection.

Results: A total of 415 microaneurysms could be analyzed in 31 eyes from 25 patients. Microaneurysms detected on single image, ×3, ×5, and ×10 averaged OCTA images were 144 (34.7%), 227 (54.7%), 285 (68.7%), and 306 (73.7%), respectively. Microaneurysm detection capability was significantly increased with increased image averaging. Microaneurysm detection with OCTA was not correlated with retinal thickness, FA leakiness, and indocyanine green angiogram detection or the number of averaged images, whereas there was significant correlation between microaneurysm morphology and microaneurysm visibility by the image-averaging process for 4 morphologies, particular the focal bulge types ($P < 0.01$).

Conclusions: In DR, multiple image averaging is useful for increasing the microaneurysm detection capability of OCTA, especially for focal bulge–type microaneurysms. *Ophthalmology Retina 2020;4:175-186 © 2019 by the American Academy of Ophthalmology*

Supplemental material available at www.ophthalmologyretina.org.

See Commentary on page 187.

In diabetic retinopathy (DR), microaneurysms are the earliest recognizable findings and their quantity could be a progression predictor,[1,2] making them clinically important features for diagnosis and follow-up. Microaneurysms can lead to extravascular leakage, resulting in diabetic macular edema (DME), which causes serious vision loss in patients with diabetes.[3] Although classic pathologic approaches have shown microaneurysms as dilations of retinal capillaries,[4] a recent study using advanced imaging techniques has demonstrated various morphologic classifications.[5]

OCT angiography (OCTA) enables detection of retinal vascular abnormality in DR at the capillary level.[6–9] However, current OCTA systems cannot image all microaneurysms.[10–13] We recently reported that microaneurysm detection in OCTA was dependent on intraaneurysmal turbulence.[14] Furthermore, Spaide et al reported that each microaneurysm image in repeated OCTA scans is different.[15] This suggests that turbulence patterns might differ between individual images.

Uji et al previously demonstrated that OCTA image averaging improves image quality in healthy volunteers because of lower background noise and greater continuity of retinal microvasculature compared with a single unaveraged image.[16,17] In this study, we investigated whether multiple image averaging could enhance microaneurysm detection capability in DR by OCTA.

Methods

Human Subjects

Humans were included in this study. This study was approved by the institutional ethics committees of the Kyushu University

© 2019 by the American Academy of Ophthalmology
Published by Elsevier Inc.

https://doi.org/10.1016/j.oret.2019.09.010
ISSN 2468-6530/19

Hospital (28-473, UMIN 000028656) and performed in accordance with the ethical standards established by the Declaration of Helsinki. Written informed consent for the research was obtained from all participants. No animal subjects were used in this study.

Patient Population

We prospectively selected 62 eyes of 31 patients with DR. Inclusion criteria on visual acuity was set at 20/32 or higher. All patients underwent OCTA examination and fundus angiography with an intravenous injection of contrast agent dye on the same day at Kyushu University Hospital between April 2018 and December 2018. We excluded eyes with any other ocular disease that might lead to microvascular disturbance in the retina or choroid (e.g., retinal vascular occlusion, age-related macular degeneration, glaucoma).

Fundus Angiography with Intravenous Dye Injection

All patients underwent fluorescein angiography (FA) and indocyanine green angiogram (IA) using Spectralis HRA-OCT (Heidelberg Engineering, Heidelberg, Germany) by simultaneous injection of these contrast agent dyes. FA and IA images for this study were selected from the early phase (within 2 minutes from dye injection) and late phase (>7 minutes from dye injection), respectively. We defined microaneurysms as hyperfluorescent dots on early-phase FA imaging as assessed by 2 independent retina specialists (YK and SN).[13] When the evaluation of the 2 observers differed, a third observer (IW) evaluated the microaneurysms.

OCT Angiography

In this study, OCTA imaging was obtained for all patients using 2 different devices (RTVue XR Avanti, Optovue Inc, Fremont, CA; and OCT-HS100, Canon Inc, Tokyo, Japan). The scanning area was a 3 × 3 mm fovea-centered region. We obtained en face OCTA images of the superficial capillary plexus (SCP) and deep capillary plexus (DCP) from each device, respectively, and low-quality images with signal strength less than 5 or images with artifacts were excluded from this study. The RTVue XR Avanti device has an A-scan rate of 70,000 scans/second, using a scan light centered at 840 nm with a bandwidth of 45 nm and a tissue resolution of 5 μm axially. Each B-scan contains 216 A-scans. Five consecutive B-scans (M-B frames) were captured at a fixed position before proceeding to the next sampling position. The segmentation line used to divide the SCP and DCP was defined as follows. For the SCP, the inner and outer boundaries were set at the inner limiting membrane and 10 μm above the inner plexiform layer (IPL), respectively. For the DCP, the inner and outer boundaries were set at 10 μm above the IPL and 10 μm below the outer plexiform layer, respectively. In contrast, the OCT-HS100 device has an A-scan rate of 70,000 scans/second and the wavelength is 855 nm. The vertical and axial resolutions were 20 μm and 3 μm, respectively. The segmentation line for the OCT-HS100 device was defined as follows. For the SCP, the inner and outer boundaries were set at the inner limiting membrane and 50 μm below the IPL, respectively. For the DCP, the inner and outer boundaries were set at 50 μm below the IPL and at the outer plexiform layer, respectively. OCTA imaging with the OCT-HS100 device was performed over 10 consecutive times for each eye, and we obtained 10 high-quality single images that satisfy the aforementioned acceptance criteria. Furthermore, a multiple en face image-averaging process using these high-quality single OCTA images was performed by image-averaging software installed on the OCT HS-100 device.[18] Finally, we obtained several types of averaged OCTA images according to the number of single OCTA images (×3, ×5, ×10) used for each averaged OCTA image.

Image Evaluation and Analysis

We obtained 5 types of OCTA images (SCP and DCP) per eye using 2 devices (i.e., single unaveraged image; ×3, ×5, and ×10 averaged image derived from the OCT HS-100 device; and a single normal scan image from the RTVue XR Avanti device) (Fig 1). Image evaluation and analysis were performed by 2-way methods (i.e., only OCTA or FA images were initially investigated with masking of the other image), which we express as "OCTA to FA analysis" and "FA to OCTA analysis," respectively. For the OCTA to FA analysis, 5 types of OCTA images were first scrutinized by 2 independent retina specialists (YK and SN) with the FA image of each eye masked; all microaneurysm-like points were detected. Based on the structural features of the microvasculature seen on the OCTA image, we defined microaneurysm-like points as focal bulge, saccular or pedunculated, fusiform, or mixed saccular/fusiform shape regions based on the report by Dubow et al.[5] All microaneurysm-like lesions detected by both retina specialists were marked on each OCTA image as a "microaneurysm-suspected point." Next, all microaneurysm-suspected points were confirmed using the corresponding early-phase FA image (Fig 2). Finally, the microaneurysm detection ratio for each type of image for each eye was respectively calculated as follows. The number of microaneurysms correctly detected on the OCTA image was divided by the total number of microaneurysms seen on the corresponding 3 × 3 mm area of the early-phase FA image. In this study, we defined microaneurysms seen in the early-phase FA image as microaneurysm. Furthermore, to investigate the impact of image averaging on microaneurysm detection capability, the 4 OCTA image types derived from the OCT HS-100 device (i.e., single unaveraged image; ×3, ×5, and ×10 averaged images) were statistically compared pair-wise by McNemar test. In contrast, the FA to OCTA analysis was performed as follows. First, early-phase FA images of each eye were assessed by a single researcher (YK) masked to the corresponding OCTA images; this researcher detected all microaneurysms present within the OCTA scan frame (3 × 3 mm). The microaneurysms were confirmed by dye leakage on late-phase FA imaging and image capture in IA imaging at the early phase. Furthermore, the mean retina thickness value (expressed as micrometers) of the ETDRS grid sector was calculated, where each microaneurysm was also evaluated by superimposing the early-phase FA image on the retina thickness map image obtained using the Cirrus HD-OCT model 5000 device (Carl Zeiss Meditec Inc, Dublin, CA) (Fig 1). Subsequently, all microaneurysms seen in the FA image at the early phase were assessed for visibility on each type of OCTA image (single unaveraged and ×3, ×5, and ×10 averaged images with the OCT HS-100 device) as a microaneurysm, and the minimum number (MN) of OCTA images for the averaging process required for microaneurysm detection was marked on each microaneurysm. The leakage from each microaneurysm in FA and the visualization in IA were assessed by 2 independent retina specialists (YK and SN) with the early-phase FA and IA images, respectively. Microaneurysm leakage is defined as previously reported: the presence of one or more microaneurysms within a surrounding area of leakage with the fluorescein signal intensity decreasing with increasing distance from the microaneurysm.[19] When the evaluation of the 2 observers differed, a third observer (IW) evaluated the leakage in FA and visualization in IA. The κ coefficient was 0.91 (95% confidence interval, 0.86 to 0.95; $P < 0.0001$) and 0.93 (95% confidence interval 0.89 to 0.96; $P < 0.0001$) for the evaluation of microaneurysm leakage in FA and

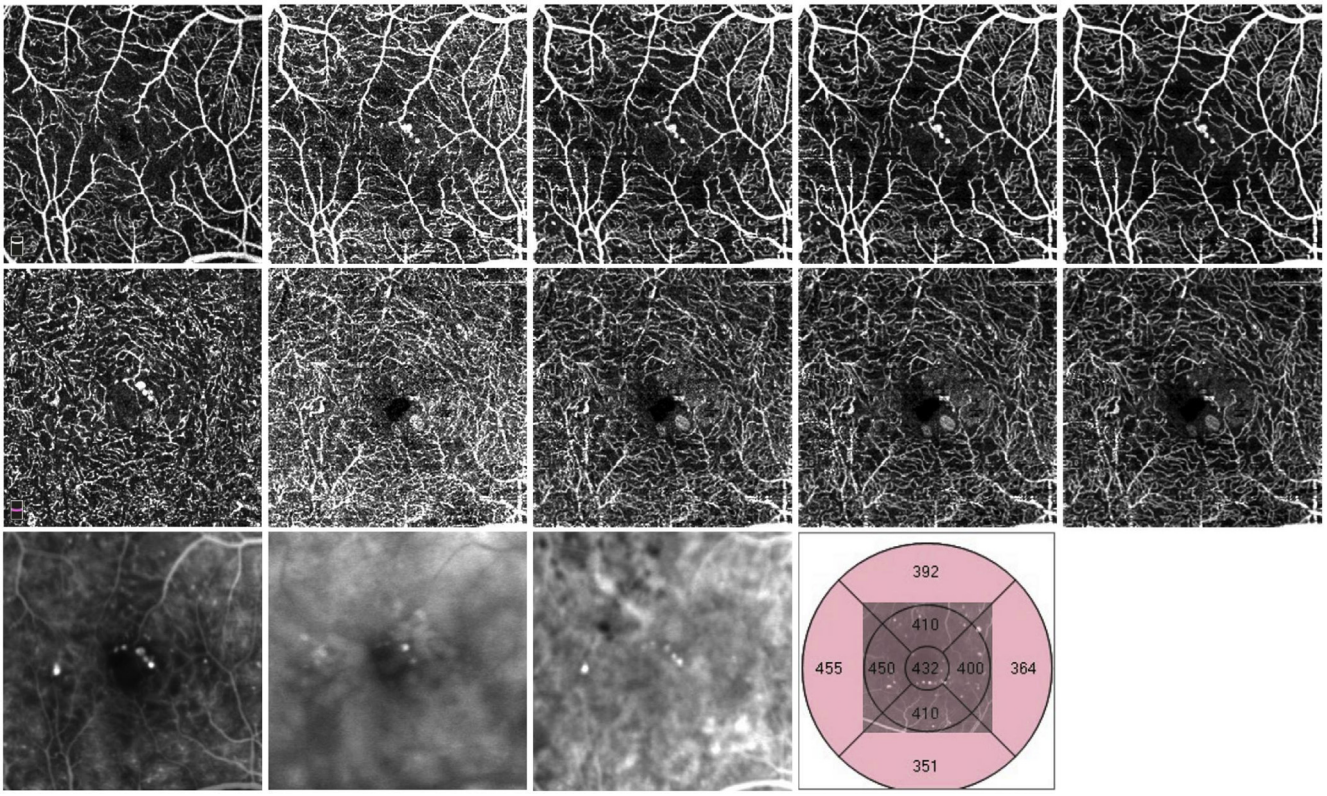

Figure 1. Representative images obtained from a right eye with severe nonproliferative diebatic retinopathy of a 44-year-old male patient. *Top row*, OCT angiography (OCTA) image of the superficial capillary plexus with a 3 × 3 mm scan frame. From left to right, normal scan image obtained by the RTVue XR Avanti device showing single unaveraged and ×3, ×5, ×10 averaged images derived from the OCT HS-100 device, respectively. *Middle row*, OCTA image of the deep capillary plexus with a 3 × 3 mm scan frame. From left to right, normal scan image obtained by the RTVue XR Avanti device showing single unaveraged and ×3, ×5, ×10 averaged images derived from the OCT HS-100 device, respectively. *Bottom row*, From left to right, early-phase and late-phase image (3 × 3 mm) of fluorescein angiography; the early phase of indocyanine green angiogram image (3 × 3 mm) and translucent early-phase fluorescein angiography image (3 × 3 mm) were superimposed on the retinal thickness map of an ETDRS grid with a diameter 6 mm.

the visualization in IA, respectively. Furthermore, all FA-detected microaneurysms visible in the ×10 averaged OCTA image were classified according to the morphology (focal bulge, saccular or pedunculated, fusiform, and mixed saccular/fusiform) based on their appearance in the ×10 averaged OCTA image. The correlation between retinal thickness value (expressed as micrometers) of the ETDRS grid sector where each microaneurysm was located and the MN of each microaneurysm was investigated by the Tukey–Kramer test. The correlation between the presence or absence of leakage from microaneurysms and the difference in its visibility in several types of unaveraged or averaged OCTA images were investigated by stratified analysis using the Breslow–Day test. We also performed the same statistical analysis for the correlation between microaneurysm visibility in IA and the difference in microaneurysm visibility in several types of unaveraged or averaged OCTA images. Furthermore, the correlation between the microaneurysm morphology classified using the ×10 averaged OCTA image and the improvement of microaneurysm visibility by the image-averaging process were investigated by chi-square testing.

Statistical Analysis

All data were expressed as the mean (standard deviation). Statistical analyses were performed using several software packages. The Tukey–Kramer and McNemar tests were performed using JMP (v. 12.0, SAS Institute, Cary, NC); the Breslow–Day test was performed using R (version.3.5.0, R Foundation for Statistical Computing, Vienna, Austria); and chi-square testing was performed using Microsoft Excel (Microsoft, Redmond, WA). Data that were not normally distributed were analyzed by nonparametric statistics. P values < 0.05 were considered statistically significant.

Results

Of the 62 eyes with DR in this study, 31 (50%) were excluded because of low image quality because of cataract, vitreous hemorrhage, poor fixation, or image artifacts. A final 31 eyes with DR (50%) of 25 patients could be analyzed (mean age, 62.0±12.6 years; 19 males and 6 females; 1 eye with mild nonproliferative DR [NPDR], 13 eyes with moderate NPDR, 9 eyes with severe NPDR, 8 eyes with proliferative DR, 13 eyes with DME).

Impact of Multiple Image Averaging on Microaneurysm Detection

OCTA to FA Analysis. We first examined the percentage of microaneurysms defined in OCTA among those detected by FA. The microaneurysm detection ratio of the OCTA scan by the RTVue XR Avanti device, and the single unaveraged, ×3, ×5, and ×10

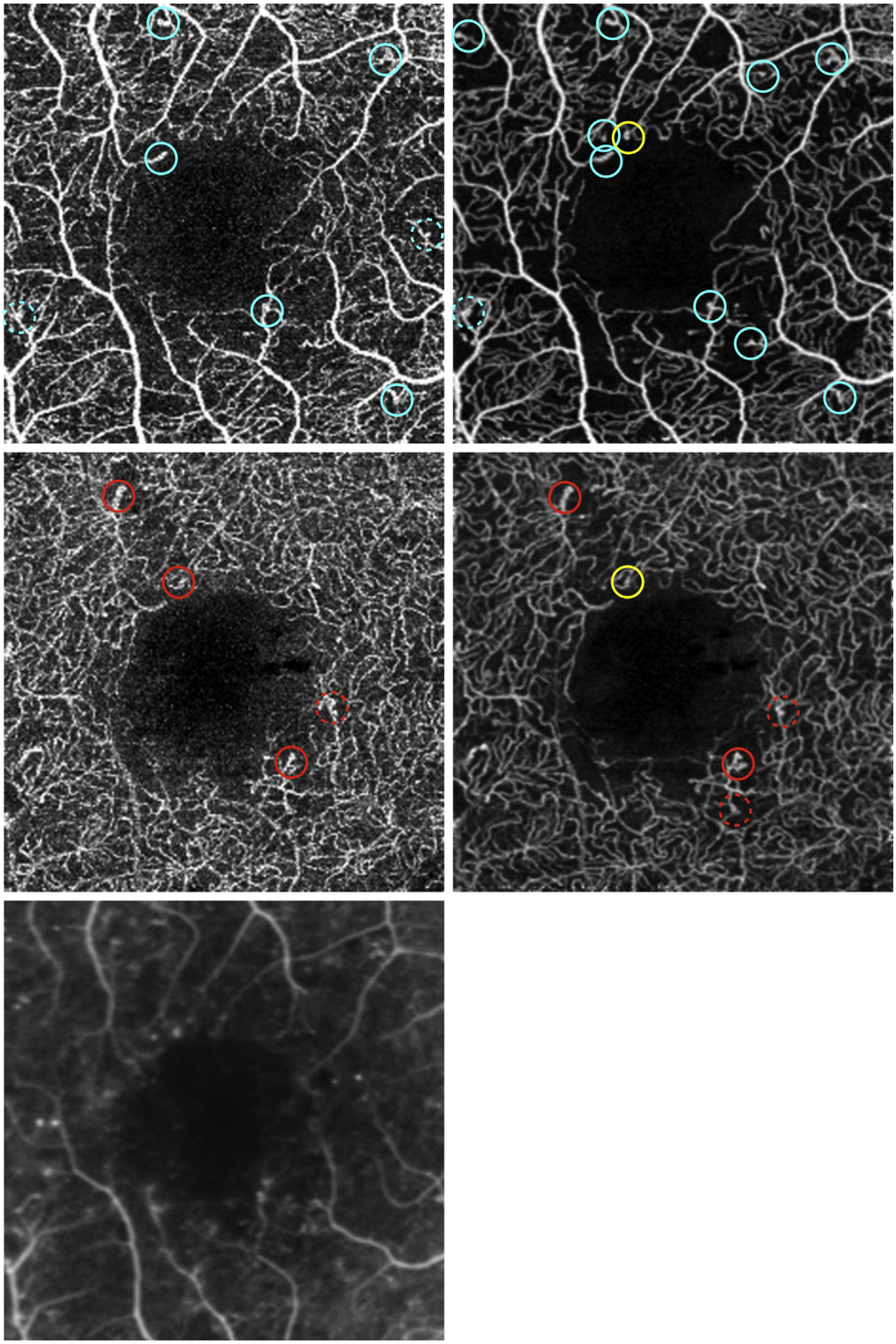

Figure 2. The methodology of OCT angiography (OCTA) to fluorescein angiography (FA) analysis. *Top row*, Single unaveraged (left) and ×10 averaged (right) OCTA images of the superficial capillary plexus (SCP) derived from the OCT HS-100 device. *Blue solid* or *dotted circles* indicate microaneurysm-suspected points detected only on SCP. *Middle row*, Single unaveraged (left) and ×10 averaged (right) OCTA images of the deep capillary plexus (DCP) derived from the OCT HS-100 device. The *red* and *yellow* circles (solid and dotted) indicate microaneurysm-suspected points detected only on the DCP and on both layers (SCP and DCP), respectively. *Bottom row*, Early-phase FA image of corresponding area of OCTA images. *Solid circles* indicate true microaneurysms, and *dotted circles* indicate false microaneurysms.

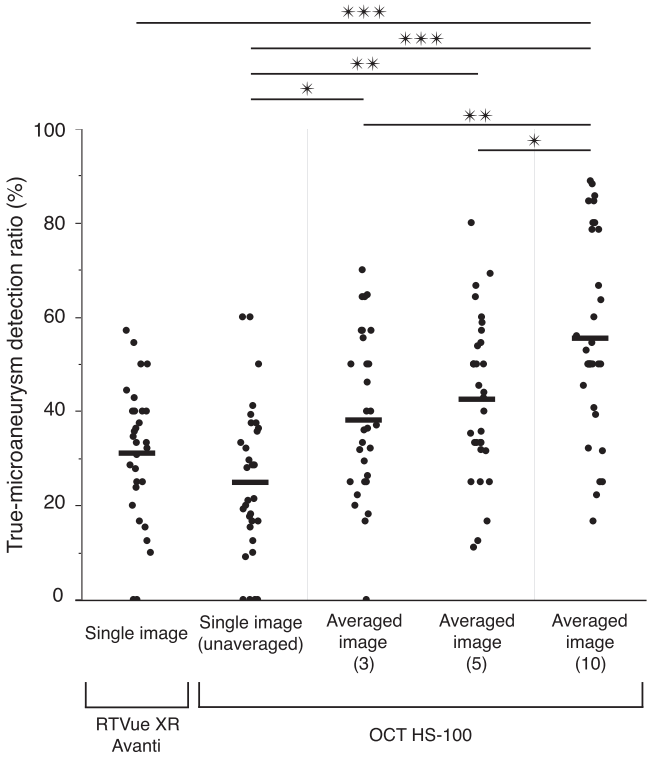

Figure 3. Comparison of the true microaneurysm detection ratio among 5 types of OCT angiography images. * $P < 0.05$, ** $P < 00.01$, ***$P < 0.001$.

averaged images derived from the OCT HS-100 device were 31.3%±14.3%, 25.0%±16.2%, 38.6±17.5%, 42.6%±17.0%, and 55.8%±21.3%, respectively (Fig 3). The microaneurysm detection ratios of the unaveraged images between the RTVue XR Avanti and OCT HS-100 devices were similar. The detection ratio with the OCT HS-100 device significantly increased as the number of single OCTA images used for averaging increased. Furthermore, the detection ratio in the ×10 averaged HS-100 image was significantly higher than with the RTVue XR Avanti device (Fig 3). We also analyzed the data with the McNemar test for confirmation. Statistical analysis indicated that the detection capabilities of the 4 types of OCTA images derived from the OCT HS-100 device significantly increased with the increasing number of single OCTA images used for averaging except for the comparison between ×3 and × 5 averaged images (Table 1).

FA to OCTA Analysis. A total of 415 microaneurysms could be observed in the 3 × 3 mm foveal areas of early-phase FA images of 31 eyes. Of these 415 microaneurysms, we next investigated whether the FA-detected microaneurysms could be imaged by OCTA. The number of microaneurysms detected in the single unaveraged image and the ×3x, ×5, and ×10 averaged OCTA images were 144 (34.7%), 227 (54.7%), 285 (68.7%), and 306 (73.7%), respectively. Detailed data for individual eyes are shown in supplemental Table S1 (available at www.ophthalmologyretina.org). The number of microaneurysms with MNs (the minimum number of OCTA image for the averaging process required for microaneurysm detection) with ×1, ×3, ×5, and ×10 were 144 (34.7%), 84 (20.2%), 59 (14.2%), and 22 (5.3%), respectively. Of the total number of microaneurysms, 106 (25.5%) were not detectable in any of the OCTA images used for analysis. Representative images of microaneurysms on OCTA with various MNs are shown in Fig 4.

Clinical Features and Visualization of Microaneurysms with Multiple Image Averaging

To consider the impact of retinal edema or the leakiness on microaneurysm visualization, we examined the relationship between these clinical features and MNs for microaneurysm detection with OCTA imaging. The retinal thickness value (in micrometers) of the ETDRS grid sector where each microaneurysm was located and the MN were not correlated (Fig 5). Although 284 microaneurysms (68.4%) and 131 microaneurysms (31.6%) were with and without dye leakage on late-phase FA image, respectively (Table 2), FA dye leakage and the MN for microaneurysm detection in OCTA image were not correlated (Table 3). Furthermore, we examined the correlation between IA visibility and the MN for microaneurysm detection in the OCTA image. Two hundred sixty-nine microaneurysms (64.8%) were visible with IA imaging, whereas 146 microaneurysms (35.2%) were invisible. Microaneurysm visibility in IA images and the difference in microaneurysm visibility in several types of unaveraged or averaged OCTA image were not correlated (Table 4).

Morphology and Visualization of Microaneurysms with Multiple Image Averaging

A previous article with adaptive optics described the morphologic classification of microaneurysms.[5] We found that detailed morphology of some microaneurysms could be observed using multiple OCTA image averaging (Fig 6). To investigate the impact

Table 1. Comparison of Microaneurysm Detection Capability (Using the McNemar Test) Among 4 Types of OCT Angiography Images Derived From the OCT HS-100 Device

Image Types		Microaneurysms Detected on Both A and B (N)	Detected Only on A (N)	Detected Only on B (N)	P Value
A	B				
Unaveraged	Averaged (×3)	77	31	86	<0.0001
Unaveraged	Averaged (×5)	83	24	90	<0.0001
Unaveraged	Averaged (×10)	80	26	131	<0.0001
Averaged (×3)	Averaged (×5)	124	38	52	0.14
Averaged (×3)	Averaged (×10)	129	36	81	<0.01
Averaged (×5)	Averaged (×10)	146	31	65	<0.001

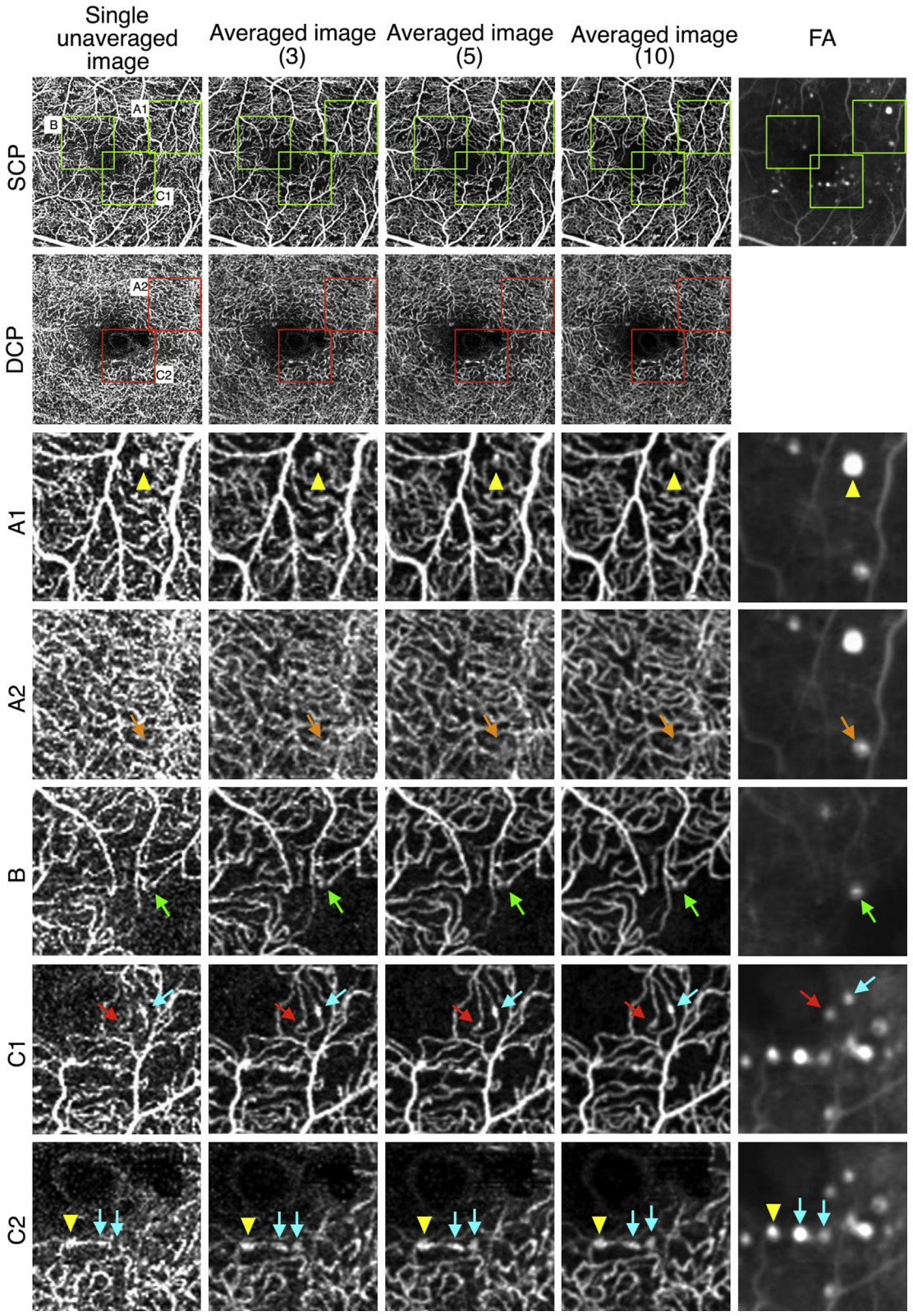

Figure 4. Representative images of microaneurysm with various minimum numbers (MNs) in an eye with moderate nonproliferative diabetic retinopathy (65-year-old male patient). Each type of OCT angiography (OCTA) image was cropped by a 1000 μm square area (**A, B,** and **C**). *Yellow arrowheads* indicate microaneurysms detected by all types of OCTA image. *Blue*, *green*, and *red arrows* indicate microaneurysms with MNs of 3, 5, and 10, respectively. *Orange arrows* indicate microaneurysms that were undetectable in all types of OCTA image. *DCP* = deep capillary plexus; *FA* = fluorescein angiography; *MN* = the minimum number of single images required for averaging to detect each microaneurysm; *SCP* = superficial capillary plexus.

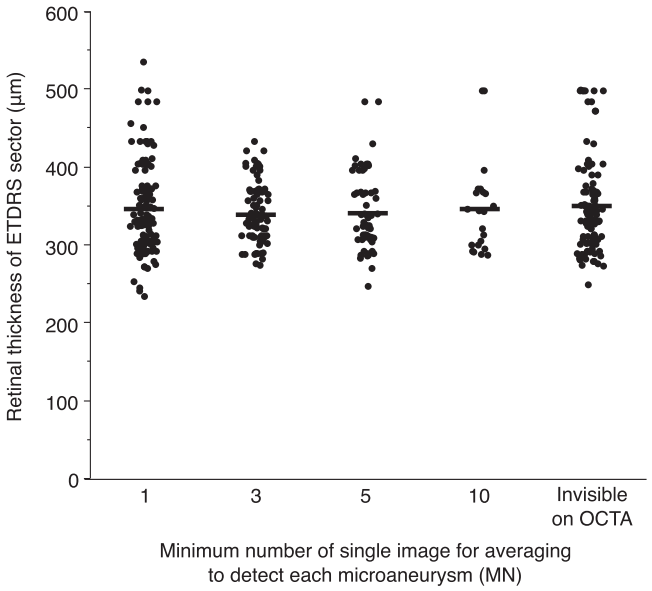

Figure 5. Correlation between retinal thickness and minimum number of single images required for averaging to detect each microaneurysm. OCTA = OCT angiography.

of microaneurysm morphology on its visualization, we classified the ×10 averaged OCTA images into 4 morphologic types. Of 306 microaneurysms detected on ×10 averaged OCTA images, 130 microaneurysms (42.5%) could be clearly classified into 4 morphologic types (Fig 6). The proportion of focal bulge microaneurysms detected without and with averaging was 27.3% and 72.7%, respectively. The proportion of microaneurysms detected with and without averaging in the other 3 groups is shown in Table 5. Statistical analysis using chi-square testing for all pairs of morphologic types showed that the proportion of visible focal bulge microaneurysms is significantly less than the proportion of the other 3 types without the image-averaging process (Table 6). However, no significant correlations were observed in comparison among the saccular or pedunculated group, the fusiform group, and the mixed group. These data indicate that OCTA averaging is significantly useful for improving the detection rate of focal bulge—type microaneurysm compared with the other 3 imaging types.

Discussion

Although OCTA imaging is useful for visualizing most diabetic retinal vascular abnormalities (e.g., neovascularization and nonperfused area),[7,11] approximately 20% to 60% of FA-detected microaneurysms could not be imaged with OCTA.[10–13] Recently, we demonstrated that microaneurysm detection by OCTA was dependent on intramicroaneurysmal turbulence.[14] Furthermore, the observation by Spaide et al on microaneurysms suggests that intramicroaneurysmal flow is intermittent.[9] These reports motivated us to investigate the utility of multiple enface OCTA image averaging on microaneurysm detection in eyes with DR. This study showed that the detection rate increased significantly as the number of images used for averaging increased to 10, suggesting the utility of OCTA image averaging on microaneurysm detection. We infer that the image-averaging process improves visualization consistency of the microvasculature, resulting in a higher detection rate of microaneurysms. However, it is unclear whether the number of averages can increase the detection rate further. In addition, some microaneurysms in this study could not be detected even with 10 high-quality images used for averaging. Because multiple averages require imaging time, a future study is necessary to investigate how many averages are useful for clinical detection of microaneurysms. We further calculated microaneurysm detection ratios of each type of OCTA image by a 2-way approach (i.e., OCTA to FA and FA to OCTA analysis). Microaneurysm detection ratios calculated from the latter approach were higher than those from the former approach. This may be due to inevitable bias.

OCTA recognizes the movement of red blood cells (RBCs) and consequently visualizes retinal vasculatures (Video S1, available at www.ophthalmologyretina.org).[20–22] Therefore, the following 4 cases can be considered as causes impeding OCTA detection of FA-detected microaneurysms (Fig 7).

1. For microaneurysms with intermittent RBC flow (Video S2, available at www.ophthalmologyretina.org), different imaging sessions may differentially detect blood flow. OCTA averaging can be useful for this even if microaneurysms coincidentally cannot be detected in a single image.
2. For microaneurysms with slower blood flow than the detection threshold (Video S3, available at www.ophthalmologyretina.org), the OCTA signal is normalized between 0 and 1, and the slowest detectable flow is determined by the interscan time in each machine.[20] Therefore, when the flow in the microaneurysm is too slow to be detected by the

Table 2. Characteristics of Microaneurysms Seen on Early-Phase Fluorescein Angiography Imagery

Characteristics	MN = 1	MN = 3	MN = 5	MN = 10	Undetectable on OCTA
Presence of leakage					
With (n = 284)	105	63	38	15	63
Without (n = 131)	39	21	21	7	43
Visibility on IA					
Visible (n = 269)	95	59	38	14	63
Invisible (n = 146)	49	25	21	8	43

IA = indocyanine green angiogram; MN = the minimum number of single OCTA images required for the averaging process to detect microaneurysms on OCTA image; OCTA = OCT angiography.

Table 3. Correlation Analysis between Leakage of Microaneurysms and Visibility on OCT Angiography Images Derived From the OCT HS-100 Device

Image Types			Microaneurysms Detected on Both A and B	Detected Only on A	Detected Only on B	Undetected on Both A and B	P Value
A	B	With or Without Leakage					
Unaveraged	Averaged (×3)	With (n = 284)	104	1	63	116	0.43
		Without (n =131)	39	0	21	71	
Unaveraged	Averaged (×5)	With (n = 284)	104	1	100	79	0.46
		Without (n = 131)	39	0	42	50	
Unaveraged	Averaged (×10)	With (n = 84)	104	1	114	65	0.46
		Without (n = 131)	39	0	49	43	
Averaged (×3)	Averaged (×5)	With (n = 284)	166	1	38	79	0.51
		Without (n = 131)	60	0	21	50	
Averaged (×3)	Averaged (×10)	With (n = 284)	166	1	52	65	0.50
		Without (n = 131)	60	0	28	43	
Averaged (×5)	Averaged (×10)	With (n = 284)	203	1	15	65	0.46
		Without (n = 131)	81	0	7	43	

P values were calculated using the Breslow-Day test.

set interscan time, OCTA cannot image the microaneurysm. Averaging is not applicable for this type of microaneurysm, and interscan time changes are necessary for their detection.[23]

3. For microaneurysms with only plasma flow but not RBCs (Video S4, available at www.ophthalmologyretina.org), it is unclear whether microaneurysms with such conditions actually exist in patients with DR. It may be possible in microaneurysms with a smaller stem vessel diameter compared with the RBC diameter in the saccular or pedunculated types as classified by Dubow et al.[5]
4. If RBCs were highly concentrated or occluded in the intramicroaneurysmal space, the flow signal of these microaneurysms might not be detected. Although these latter cases cannot be excluded, we speculate that these microaneurysms would be undetectable on both OCTA and FA.

In this study, we examined the correlation between the clinical features of FA leakage, IA visualization ability, and retinal thickness, and improvement in visualization ability by averaging, but no correlations were found. This may suggest that OCTA averaging is also effective for leaky microaneurysms or microaneurysms in edema. We previously reported that no correlation was observed between intramicroaneurysmal turbulence and leakage from microaneurysms.[14] Endothelial barrier disruption, which is a cause of vascular leakage, may not correlate with the degree of intramicroaneurysmal turbulence.

Interestingly, the detection rate of focal bulge–type microaneurysms was lower than the other types in unaveraged images, and the detection rate with image averaging was significantly higher (improved). As the visualization with OCTA depends on intraaneurysmal flow,[14] these data might indicate that turbulence may be intermittent in focal bulge microaneurysms. The

Table 4. Correlation Analysis between Visibility of Microaneurysms on Indocyanine Green Angiogram Images and Visibility on OCT Angiography Images Derived from the OCT HS-100 Device

Image Types			Microaneurysms Detected on Both A and B	Detected Only on A	Detected Only on B	Undetected on Both A and B	P Value
A	B	Visibility on IA					
Unaveraged	Averaged (×3)	Visible (n = 269)	95	0	59	115	0.22
		Invisible (n = 146)	48	1	25	72	
Unaveraged	Averaged (×5)	Visible (n = 269)	95	0	96	78	0.22
		Invisible (n = 146)	48	1	46	51	
Unaveraged	Averaged (×10)	Visible (n = 269)	95	0	110	64	0.23
		Invisible (n = 146)	48	1	53	44	
Averaged (×3)	Averaged (×5)	Visible (n = 269)	153	1	38	77	0.48
		Invisible (n = 146)	73	0	21	52	
Averaged (×3)	Averaged (×10)	Visible (n = 269)	153	1	52	63	0.43
		Invisible (n = 146)	73	0	28	45	
Averaged (×5)	Averaged (×10)	Visible (n = 269)	191	0	14	64	0.22
		Invisible (n = 146)	93	1	8	44	

IA = Indocyanine green angiogram.
P values were calculated using the Breslow-Day test.

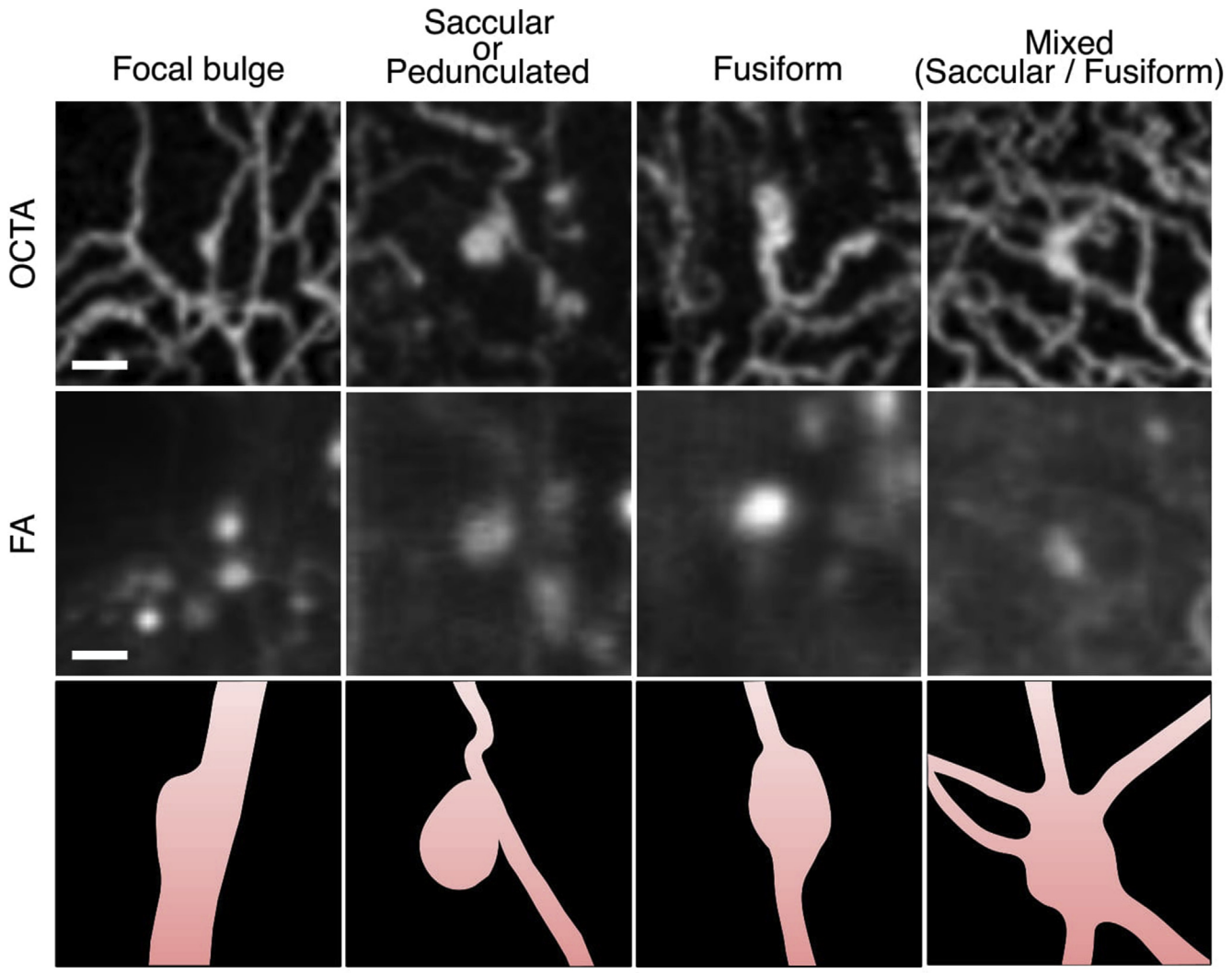

Figure 6. Morphologic classification of microaneurysms using ×10 averaged OCT angiography (OCTA) images. *Top row*, Representative images of ×10 averaged OCTA images that show 4 microaneurysm morphologies. From left to right, microaneurysms with focal bulge, saccular or pedunculated, fusiform, and mixed (saccular/fusiform) morphology are shown, respectively. *Middle row*, Early-phase fluorescein angiography (FA) image of the area corresponding to the ×10 averaged OCTA images. *Bottom row*, Illustrated examples corresponding to OCTA images. Scale bars indicate 100 μm.

Table 5. Classification of Microaneurysms Based on Morphological Feature and Visibility on Unaveraged and Averaged OCT Angiography Images Derived from the OCT HS-100 Device

Morphologic Type of Microaneurysm	Detectable on Unaveraged OCTA (MN = 1)	Detectable on Averaged OCTA (MN = 3, 5, and 10)
Focal bulge	6 (27.3%)	16 (72.7%)
Saccular or pedunculated	25 (78.1%)	7 (21.9%)
Fusiform	30 (75.0%)	10 (25.0%)
Mixed (saccular/fusiform)	22 (61.1%)	14 (38.9%)

Percentages in parentheses represent the proportion of microaneurysms in each group.
MN = Minimum number; OCTA = OCT angiography.

focal bulge—type microaneurysm may have no abnormal flow because its size is smaller than other types.[5] It has previously been reported that there is a correlation between the morphology of the abdominal or intracranial aneurysm and its rupture.[24,25] Our results indicate that the morphology of a microaneurysm affects its visualization by OCTA imaging. Multiple image-averaging OCTA may be useful to reveal the clinical significance of the morphology.

Uji et al examined the utility of OCTA averaging using Image J software (Wayne Rasband, National Institutes of Health, Bethesda, MD),[17] but we used the software built into commercially available OCTA, as reported previously.[18] Marukawa et al reported that noise reduction

Table 6. Correlation between Microaneurysm Morphology and Improvement in Visibility by Image-Averaging Process

Microaneurysm Morphology		*P* Value
Focal bulge	Saccular or pedunculated	<0.001
Focal bulge	Fusiform	<0.001
Focal bulge	Mixed (saccular/fusiform)	0.01
Saccular or Pedunculated	Fusiform	0.76
Saccular or Pedunculated	Mixed (saccular/fusiform)	0.13
Fusiform	Mixed (saccular/fusiform)	0.19

P values were calculated using chi-square testing.

was observed when evaluating the utility of image averaging in cases of choroidal neovascularization (CNV) without affecting the area of CNV.[18] This study demonstrates that OCTA averaging improves both image quality and microaneurysm detection. Although noise reduction is one factor for the improvement, this may suggest that the blood flow in microaneurysms is not constant, unlike in CNV as previously mentioned.

Our study has several limitations. First, the sample size was limited. Second, patients with poor visual acuity were excluded despite some patients with DR or DME who had severe vision loss. Third, the field of view was small (3 × 3 mm), although some microaneurysms could be observed in the peripheral retina. Fourth, there was incomplete morphologic classification of microaneurysms based on 2-dimensional en face images. Thus, precise classification may be difficult because each microaneurysm is 3-dimensional. Fifth, we included patients with previous treatment for DME (e.g., anti−vascular endothelial grown factor therapy or vitrectomy despite no recent treatment). These previous treatments may affect the degree of leakage from microaneurysms or intramicroaneurysmal blood flow. Future study is necessary to investigate whether these treatments can affect the improvement of microaneurysm detection capability by OCTA averaging.

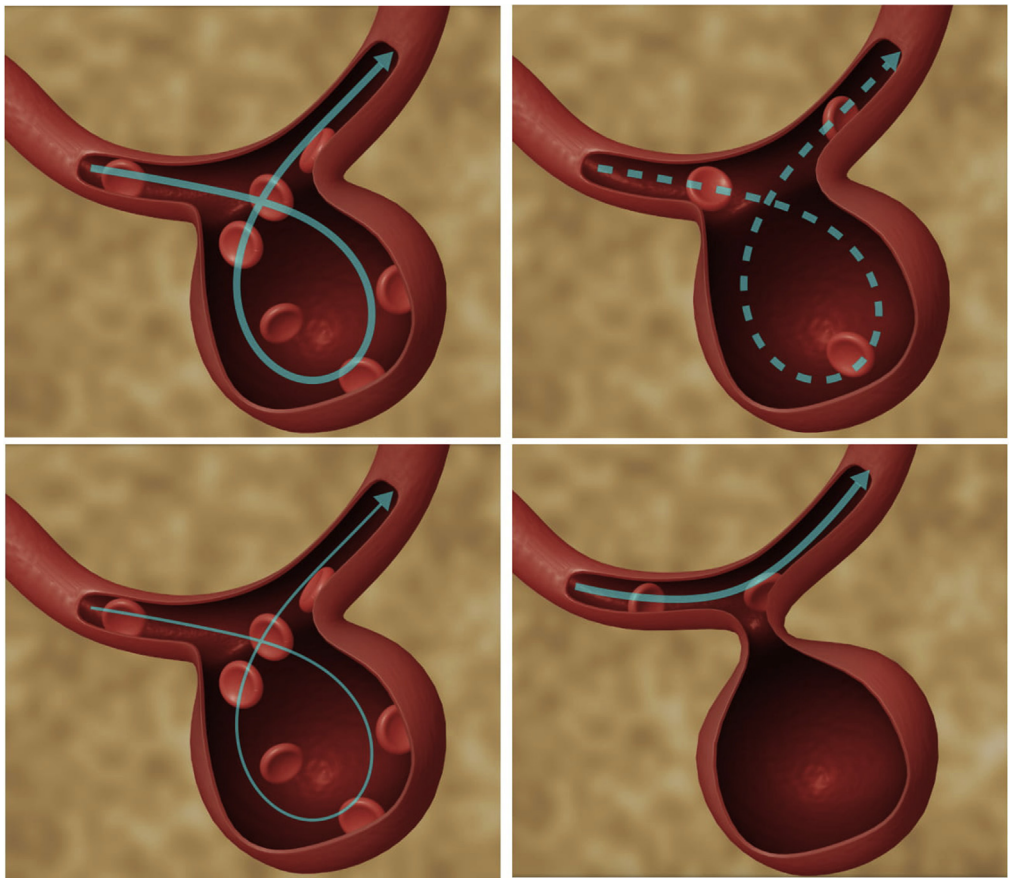

Figure 7. A hypothesized model of microaneurysm detection by OCT angiography (OCTA) multiple image averaging. Microaneurysms detection by OCTA could depend on intraaneurysmal turbulence (*top left*). However, part of the fluorescein angiography−detected microaneurysms cannot be detected by OCTA. Three possible microaneurysm cases contribute to nondetection by OCTA: (1) microaneurysms with intermittent red blood cell (RBC) flow (*top right*); (2) microaneurysms with blood flow slower than detection threshold (*bottom left*); (3) microaneurysms with only plasma flow but not RBCs (*bottom right*).

Acknowledgment. We thank Juun Horie (Canon Inc) for his technical support.

References

1. Klein R, Meuer SM, Moss SE, Klein BE. The relationship of retinal microaneurysm counts to the 4-year progression of diabetic retinopathy. *Arch Ophthalmol*. 1989;107:1780−1785.
2. Kohner EM, Stratton IM, Aldington SJ, et al. Microaneurysms in the development of diabetic retinopathy (UKPDS 42). UK Prospective Diabetes Study Group. *Diabetologia*. 1999;42:1107−1112.
3. Murakami T, Nishijima K, Sakamoto A, et al. Foveal cystoid spaces are associated with enlarged foveal avascular zone and microaneurysms in diabetic macular edema. *Ophthalmology*. 2011;118:359−367.
4. Cogan DG, Toussaint D, Kuwabara T. Retinal vascular patterns. IV. Diabetic retinopathy. *Arch Ophthalmol*. 1961;66:366−378.
5. Dubow M, Pinhas A, Shah N, et al. Classification of human retinal microaneurysms using adaptive optics scanning light ophthalmoscope fluorescein angiography. *Invest Ophthalmol Vis Sci*. 2014;55:1299−1309.
6. Kaizu Y, Nakao S, Arima M, et al. Capillary dropout is dominant in deep capillary plexus in early diabetic retinopathy in optical coherence tomography angiography. *Acta Ophthalmol*. 2019;97:e811−e812.
7. Kaizu Y, Nakao S, Sekiryu H, et al. Retinal flow density by optical coherence tomography angiography is useful for detection of nonperfused areas in diabetic retinopathy. *Graefes Arch Clin Exp Ophthalmol*. 2018;256:2275−2282.
8. Kaizu Y, Nakao S, Yoshida S, et al. Optical coherence tomography angiography reveals spatial bias of macular capillary dropout in diabetic retinopathy. *Invest Ophthalmol Vis Sci*. 2017;58:4889−4897.
9. Spaide RF, Fujimoto JG, Waheed NK. Optical coherence tomography angiography. *Retina*. 2015;35:2161−2162.
10. Miwa Y, Murakami T, Suzuma K, et al. Relationship between functional and structural changes in diabetic vessels in optical coherence tomography angiography. *Sci Rep*. 2016;6:29064.
11. Ishibazawa A, Nagaoka T, Takahashi A, et al. Optical coherence tomography angiography in diabetic retinopathy: a prospective pilot study. *Am J Ophthalmol*. 2015;160:35−44.e1.
12. Hasegawa N, Nozaki M, Takase N, et al. New insights into microaneurysms in the deep capillary plexus detected by optical coherence tomography angiography in diabetic macular edema. *Invest Ophthalmol Vis Sci*. 2016;57:348−355.
13. Couturier A, Mane V, Bonnin S, et al. Capillary plexus anomalies in diabetic retinopathy on optical coherence tomography angiography. *Retina*. 2015;35:2384−2391.
14. Nakao S, Yoshida S, Kaizu Y, et al. Microaneurysm detection in diabetic retinopathy using OCT angiography may depend on intramicroaneurysmal turbulence. *Ophthalmology Retina*. 2018;2:1171−1173.
15. Spaide RF, Fujimoto JG, Waheed NK. Image artifacts in optical coherence tomography angiography. *Retina*. 2015;35:2163−2180.
16. Uji A, Balasubramanian S, Lei J, et al. Multiple enface image averaging for enhanced optical coherence tomography angiography imaging. *Acta Ophthalmol*. 2018;96:e820−e827.
17. Uji A, Balasubramanian S, Lei JB, et al. Impact of multiple en face image averaging on quantitative assessment from optical coherence tomography angiography images. *Ophthalmology*. 2017;124:944−952.
18. Murakawa S, Maruko I, Kawano T, et al. Choroidal neovascularization imaging using multiple en face optical coherence tomography angiography image averaging. *Graefes Arch Clin Exp Ophthalmol*. 2019;257:1119−1125.
19. Classification of diabetic retinopathy from fluorescein angiograms. ETDRS report number 11. Early Treatment Diabetic Retinopathy Study Research Group. *Ophthalmology*. 1991;98(5 suppl):807−822.
20. Spaide RF, Fujimoto JG, Waheed NK, et al. Optical coherence tomography angiography. *Prog Retin Eye Res*. 2018;64:1−55.
21. Wang RK, Jacques SL, Ma Z, et al. Three dimensional optical angiography. *Opt Express*. 2007;15:4083−4097.
22. Jia Y, Tan O, Tokayer J, et al. Split-spectrum amplitude-decorrelation angiography with optical coherence tomography. *Opt Express*. 2012;20:4710−4725.
23. Ploner SB, Moult EM, Choi W, et al. Toward quantitative optical coherence tomography angiography: visualizing blood flow speeds in ocular pathology using variable interscan time analysis. *Retina*. 2016;36(suppl 1):S118−S126.
24. Siegel CL, Cohan RH, Korobkin M, et al. Abdominal aortic aneurysm morphology: CT features in patients with ruptured and nonruptured aneurysms. *AJR Am J Roentgenol*. 1994;163:1123−1129.
25. Hademenos GJ, Massoud TF, Turjman F, Sayre JW. Anatomical and morphological factors correlating with rupture of intracranial aneurysms in patients referred for endovascular treatment. *Neuroradiology*. 1998;40:755−760.

Footnotes and Financial Disclosures

Originally received: June 25, 2019.
Final revision: August 27, 2019.
Accepted: September 20, 2019.
Available online: September 27, 2019. Manuscript no. ORET-D-19-00011.

[1] Department of Ophthalmology, Graduate School of Medical Sciences, Kyushu University, Fukuoka, Japan.

[2] Department of Research and Development of Next Generation Medicine, Graduate School of Medical Sciences, Kyushu University, Fukuoka, Japan.

Financial Support: This study was supported by grants from the Japan Society for the Promotion of Science KAKENHI, Grant-in-Aid for Scientific Research (C) (grant no. 17K11456 [S.N.]); the Charitable Trust Fund for Ophthalmic Research in Commemoration of Santen Pharmaceutical's Founder (S.N.); Novartis Pharmaceuticals research grants (S.N.); Alcon research grants (S.N.); Bayer Retina Award (S.N.); and the Takeda Science Foundation (S.N.).

HUMAN SUBJECTS: Human subjects were included in this study. The human ethics committees at Kyorin University School of Medicine approved the study. All research adhered to the tenets of the Declaration of Helsinki. All participants provided informed consent.

No animal subjects were included in this study.

Author contributions:

Conception and design: Kaizu, Nakao

Analysis and interpretation: Kaizu, Nakao, Akiyama, Kishimoto, Hisatomi

Data collection: Kaizu, Nakao, Wada, Arima, Yamaguchi, Ishikawa

Obtained funding: Nakao

Overall responsibility: Nakao, Sonoda

Abbreviations and Acronyms:
CNV = choroidal neovascularization; **DME** = diabetic macular edema; **DCP** = deep capillary plexus; **DR** = diabetic retinopathy; **FA** = fluorescein angiography; **IA** = indocyanine green angiogram; **IPL** = inner plexiform layer; **MN** = minimum number; **NPDR** = nonproliferative diabetic neuropathy; **OCTA** = OCT angiography; **RBC** = red blood cell; **SCP** = superficial capillary plexus.

Correspondence:
Shintaro Nakao, MD, PhD, Kyushu University, 3-1-1 Maidashi Higashi-ku, Fukuoka 812 8582, Japan. E-mail: snakao@med.kyushu-u.ac.jp.

Pictures & Perspectives

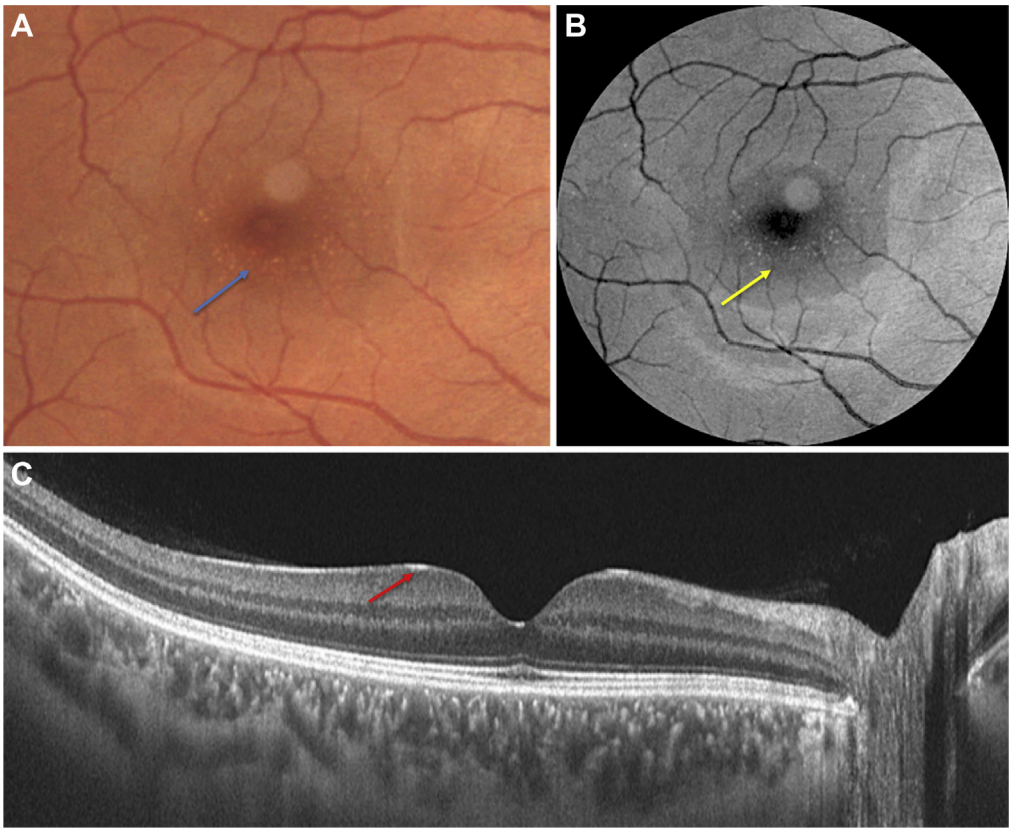

White Dot Fovea

A 33-year-old man was seen for routine examination. The anterior segment was normal in both eyes. Fundus examination revealed multiple, small, yellow dots around foveola in a ring like pattern (more dense inferiorly) in both eyes (**A**). The white dots were more prominently seen on red free images as bright dots (**B**). Swept source OCT through these dots revealed slight hyperreflectivity on the inner surface of retina (**C**). A diagnosis of bilateral white dot fovea was made and patient was reassured. White dot fovea was first described in 1997 and has been reported rarely. White dot fovea is usually more evident in darkly pigmented fundi. Clinical significance of this normal condition lies in its identification and avoiding further investigations.

Vinod Kumar, MS
Shoryavardhan Azad, MD
Pulak Agarwal, MD

Rajendra Prasad Center, All India Institute of Medical Sciences, New Delhi, India